JACS
JOURNAL OF THE AMERICAN CHEMICAL SOCIETY
Communication
pubs.acs.org/JACS

NAD$^+$ as a Hydride Donor and Reductant

Yamin Htet[†] and Andrew G. Tennyson*[,†,‡,§]

[†]Departments of Chemistry and [‡]Materials Science and Engineering, Clemson University, Clemson, South Carolina 29634, United States

[§]Center for Optical Materials Science and Engineering Technologies, Anderson, South Carolina 29625, United States

Supporting Information

ABSTRACT: Reduced nicotinamide adenine dinucleotide (NADH) can generate a ruthenium−hydride intermediate that catalyzes the reduction of O_2 to H_2O_2, which endows it with potent anticancer properties. A catalyst that could access a Ru−H intermediate using oxidized nicotinamide adenine dinucleotide (NAD$^+$) as the H$^-$ source, however, could draw upon a supply of reducing equivalents 1000-fold more abundant than NADH, which would enable significantly greater H_2O_2 production. Herein, it is demonstrated, using the reduction of ABTS$^{\bullet-}$ to ABTS^{2-}, that NAD$^+$ can function as a reductant. Mechanistic evidence is presented that suggests a Ru−H intermediate is formed via β-hydride elimination from a ribose subunit in NAD$^+$. The insight gained from the heretofore unknown ability of NAD$^+$ to function as a reductant and H$^-$ donor may lead to undiscovered biological carbohydrate oxidation pathways and new chemotherapeutic strategies.

Redox reactions provide the chemical motive force essential for all forms of life.[1,2] Reduced nicotinamide adenine dinucleotide (NADH) supplies two e^- to mitochondrial electron transport by donating H$^-$ from its hydropyridine moiety (Scheme 1, blue box) to flavin mononucleotide.[3,4] Conversely, oxidized nicotinamide adenine dinucleotide (NAD$^+$) accepts two e^- from glyceraldehyde-3-phosphate or lactate dehydrogenase by accepting H$^-$ into its pyridinium moiety (Scheme 1, purple box).[5,6] The H$^-$ donating ability of NADH has been harnessed for catalytic applications ranging from the reduction of O_2 to cytotoxic H_2O_2 in cancer cells[7−9] to petroleum-free H_2 production[10] to alcohol deracemization.[11]

Scheme 1. Hydride Transfer with NADH and NAD$^+$

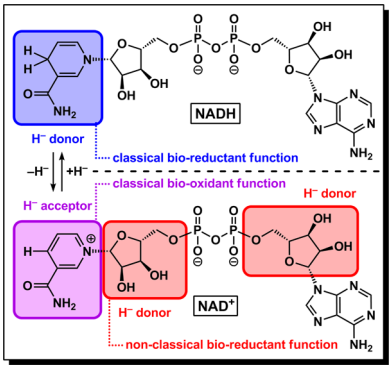

Free NAD$^+$ is 640−1100 times more abundant in cells than free NADH;[12−15] therefore, a catalyst that could utilize NAD$^+$ would have access to a significantly greater H$^-$/e^- supply than NADH. Because catalytic carbohydrate oxidation can be performed by enzymatic[16] and transition metal-based systems,[17,18] we reasoned that oxidation of a ribose subunit (Scheme 1, red boxes) could enable NAD$^+$ to function as a reductant. Catalytic oxidation of ribose has been achieved by a Ru complex to afford ribonolactone with concomitant H_2 transfer to an alkene.[19] We therefore hypothesized that (1) a ribose subunit in NAD$^+$ could similarly undergo oxidation by a Ru complex via some form of H$^-$ transfer to the metal center and (2) the resulting Ru−H species would exhibit catalytic reduction activity. Herein, we report the first instance of H$^-$ donation via β-hydride elimination from a ribose subunit of NAD$^+$, which enables NAD$^+$ to function as a reductant.

To probe for Ru−H formation, the conversion of 2,2′-azino-bis(3-ethylbenzothiazoline-6-sulfonate) radical monoanion (ABTS$^{\bullet-}$, Scheme 2A) to ABTS^{2-} was selected as a spectroscopically more convenient reduction reaction than the conversion of O_2 to H_2O_2, given that ABTS$^{\bullet-}$ consumption can be quantified at significantly lower concentrations and longer wavelengths than H_2O_2 production.[20−23] Furthermore, the reduction of ABTS$^{\bullet-}$ to ABTS^{2-} (0.68 V vs NHE)[24] occurs at nearly the same potential as the reduction of O_2 to H_2O_2 (0.70 V vs NHE).[25]

Scheme 2. Ru1-Catalyzed ABTS$^{\bullet-}$ Reduction with Alcohols

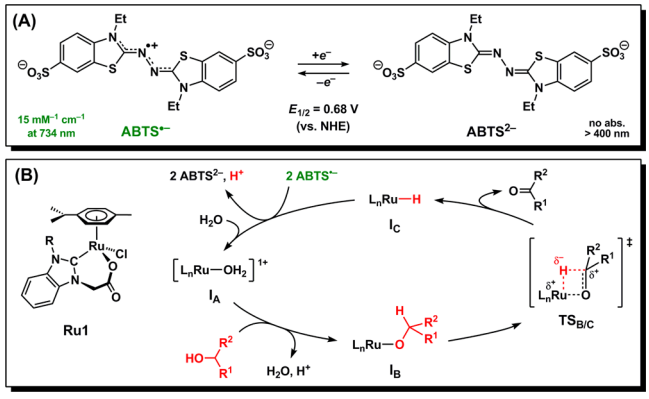

Received: October 5, 2016
Published: November 30, 2016

DOI: 10.1021/jacs.6b10451
J. Am. Chem. Soc. 2016, 138, 15833−15836

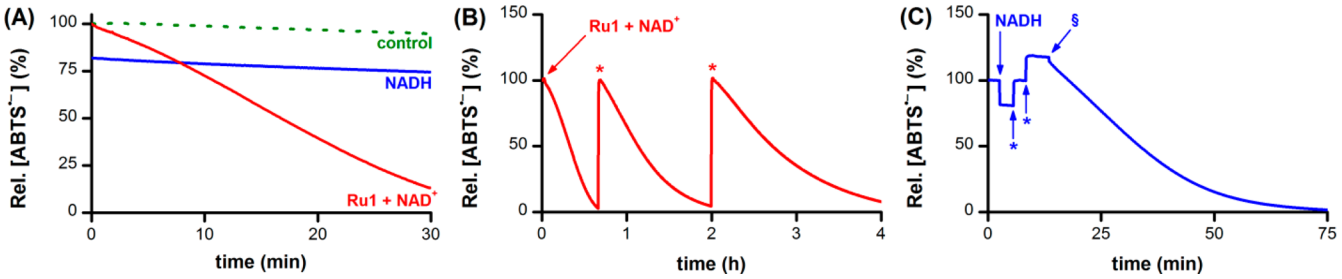

Figure 1. Plot of relative [ABTS$^{\bullet-}$] vs time, which shows the reduction of ABTS$^{\bullet-}$ to ABTS^{2-} following (A) the addition of **Ru1** and NAD$^+$ (red line), NADH (blue line), or **Ru1** without NAD$^+$ as a control (dotted green line), (B) two additional 50 μM ABTS$^{\bullet-}$ aliquots (*) after the initial reduction by **Ru1** and NAD$^+$, or (C) two additional 10 μM ABTS$^{\bullet-}$ aliquots (*) after the initial reduction by NADH, followed by **Ru1** and NAD$^+$ (§). Conditions: [**Ru1**]$_0$ or [NADH]$_0$ = 5 μM, [ABTS$^{\bullet-}$]$_0$ = 50 μM, [NAD$^+$]$_0$ = 25 mM, PBS (pH 7.4), 25 °C.

Therefore, from a thermodynamic perspective, the reactivity of Ru−H with ABTS$^{\bullet-}$ can provide insight into its reactivity with O_2.

We recently reported the catalytic reduction of ABTS$^{\bullet-}$ to ABTS^{2-} in aqueous solution using biologically relevant alcohols as terminal reductants, including arabinose, a diastereomer of ribose (Scheme 2B).[26] Subsequent kinetic studies elucidated the mechanism: in aqueous solution, **Ru1** converts to Ru−aquo complex $\mathbf{I_A}$, followed by ligand exchange with a nontertiary alcohol (R^1−CHOH−R^2) and deprotonation to afford Ru−alkoxide species $\mathbf{I_B}$, which then undergoes β-hydride elimination ($\mathbf{TS_{B/C}}$) to generate the catalytically active Ru−H intermediate $\mathbf{I_C}$ that reduces ABTS$^{\bullet-}$.[27] We reasoned that a ribose subunit of NAD$^+$ could likewise undergo β-hydride elimination to produce $\mathbf{I_C}$, whose presence could be inferred from the reduction of ABTS$^{\bullet-}$ to ABTS^{2-}.

Addition of 5 μM **Ru1** to 50 μM ABTS$^{\bullet-}$ in phosphate buffered saline (PBS, pH 7.4) followed by the addition of 25 mM NAD$^+$ produced an 87% decrease in radical absorbance within 30 min (Figure 1A, red line) that was 100% complete within 45 min. The UV/vis spectrum after 45 min confirmed a 1:1 correlation between ABTS$^{\bullet-}$ consumed and ABTS^{2-} produced (Figure S1). Attempts to characterize the NAD$^+$ oxidation product were unsuccessful, due to the low concentration constraints of the ABTS$^{\bullet-}$ reduction reaction, but calorimetric and computational studies by others suggest that dehydrogenation of the −CHOH− moiety at the ribose 2′-position would be thermodynamically the most favorable.[28,29] No radical reduction occurred in the presence of 5 μM **Ru1** alone (Figure 1A, green line), which revealed that **Ru1** by itself could not reduce ABTS$^{\bullet-}$. Similarly, no ABTS$^{\bullet-}$ reduction was observed in the absence of **Ru1**, even with NAD$^+$ concentrations as high as 50 mM, which demonstrated that NAD$^+$ by itself could not reduce ABTS$^{\bullet-}$. However, addition of 5 μM NADH produced a rapid (within mixing time) 18% decrease in radical absorbance (Figure 1A, blue line), consistent with NADH functioning as a two e^- reductant. After the initial decrease, no additional ABTS$^{\bullet-}$ reduction was observed beyond normal thermal decay.

To determine if **Ru1** remained catalytically active after the reduction of 10 equiv of ABTS$^{\bullet-}$, two subsequent aliquots of 50 μM ABTS$^{\bullet-}$ were added (*) and [ABTS$^{\bullet-}$] decreased to zero each time (Figure 1B). The time necessary for complete ABTS$^{\bullet-}$ reduction increased with each successive aliquot due to the fact that ABTS^{2-} inhibits **Ru1**-catalyzed ABTS$^{\bullet-}$ reduction.[27] After the initial decrease produced by NADH, however, addition of 10 μM ABTS$^{\bullet-}$ aliquots (*) only increased absorbance proportional to the [ABTS$^{\bullet-}$] in each aliquot (Figure 1C), which indicated that the reducing ability of NADH had been exhausted. Treatment of this solution containing 60 μM ABTS$^{\bullet-}$ with 5 μM **Ru1** and 25 mM NAD$^+$ (§), produced complete ABTS$^{\bullet-}$ reduction within 1 h.

The ability of **Ru1** to catalyze ABTS$^{\bullet-}$ reduction was assayed with the individual components of NAD$^+$: nicotinamide, adenine, and ribose. No ABTS$^{\bullet-}$ reduction occurred upon treatment of 50 μM ABTS$^{\bullet-}$ and 5 μM **Ru1** with either 25 mM nicotinamide or 1.0 mM adenine, which indicated that neither component afforded NAD$^+$ its terminal reductant ability. In contrast, the addition of 25 mM D-ribose or 1.0 mM D-ribose phosphate produced complete ABTS$^{\bullet-}$ reduction within 20 min (Figures S2−S3). The faster reactivity with D-ribose phosphate is consistent with the higher affinity of cationic $\mathbf{I_A}$ for anionic D-ribose phosphate than for neutral D-ribose. Collectively, these results demonstrated that the terminal reductant function of NAD$^+$ is derived from its ribose subunits.

The kinetics of **Ru1**-catalyzed ABTS$^{\bullet-}$ reduction with NAD$^+$ were analyzed for consistency with the mechanism in Scheme 2. Increasing the solution pH led to faster ABTS$^{\bullet-}$ reduction, with no reduction observed in pure H_2O (Figure S4), which indicated that H^+ dissociation was necessary and was consistent with the conversion of $\mathbf{I_A}$ to $\mathbf{I_B}$. Varying the reaction temperature revealed $\Delta S^{\ddagger} = 17.1 \pm 4.9$ cal mol^{-1} K^{-1} (Figure S5), which demonstrated that disorder was increasing during the rate-determining step and suggested ligand fragmentation and dissociation (i.e., $\mathbf{TS_{B/C}}$ and R^1−C(=O)−R^2 elimination, respectively) was occurring. The $\Delta S^{\ddagger}$ value observed with NAD$^+$ also fell within the range of values measured for **Ru1**-catalyzed ABTS$^{\bullet-}$ reduction with other nontertiary alcohols ($\Delta S^{\ddagger}$ = 11.4−32.8 cal mol^{-1} K^{-1}).[27] Collectively, these results were consistent with the formation of $\mathbf{I_C}$ via β-hydride elimination from a ribose subunit coordinated to Ru and dissociation of the oxidized NAD$^+$.

The observed rate constant (k_{obs}) for **Ru1**-catalyzed ABTS$^{\bullet-}$ reduction with NAD$^+$ was 2.53-fold lower in deutero PBS (pD 7.4) than in proteo PBS. This ABTS$^{\bullet-}$ reduction reaction exhibits a solvent kinetic isotope effect (KIE) of 1.74, which reflects the role of H_2O as an H^+ acceptor in the conversion of $\mathbf{I_A}$ to $\mathbf{I_B}$ and $\mathbf{I_C}$ back to $\mathbf{I_A}$.[27] Dividing the proteo/deutero k_{obs} ratio of 2.53 by 1.74 yielded the O−H/D KIE value of 1.45 for NAD$^+$. Breakage of an O−H bond in a ribose subunit of NAD$^+$ is essential for the formation of $\mathbf{I_B}$, whereby H/D substitution causes the activation barrier to increase and the k_{obs} for ABTS$^{\bullet-}$ reduction to decrease. In our previous mechanistic study, the smaller O−H/D KIE value for EtOH (2.92) compared to *i*-PrOH (4.18) reflected the lower pK_a of EtOH (15.9 vs 16.5 for *i*-PrOH).[27] Increasing the acidity of the O−H group will increase the $O^{\delta-}$−$H^{\delta+}$ bond polarization, which will lower the activation barrier to H^+ dissociation and thus render the O−H bond less

DOI: 10.1021/jacs.6b10451
J. Am. Chem. Soc. 2016, 138, 15833−15836

sensitive to H/D isotopic substitution. The substantially lower O−H/D KIE value for NAD^+ compared to EtOH and *i*-PrOH was thus consistent with the substantially greater acidity of ribose (pK_a = 11.8).[30]

We next sought to demonstrate that NAD^+ could serve as a reductant under conditions in which the biological supply of NADH had been exhausted. Treatment of a 50 μM $ABTS^{\bullet-}$ solution (Figure 2, *i*) with 18 μM NADH caused a rapid (within

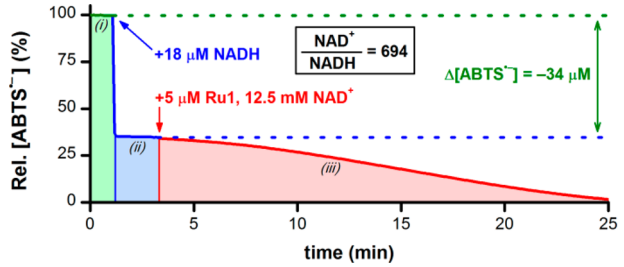

Figure 2. Plot of relative $[ABTS^{\bullet-}]$ vs time (*i*), which shows the 2:1 stoichiometric reduction of $ABTS^{\bullet-}$ by NADH (*ii*), followed by the catalytic reduction of $ABTS^{\bullet-}$ by **Ru1** and NAD^+ (*iii*). Conditions: $[\mathbf{Ru1}]_0$ = 5 μM, or $[NADH]_0$ = 18 μM, $[ABTS^{\bullet-}]_0$ = 50 μM, $[NAD^+]_0$ = 12.5 mM, PBS (pH 7.4), 25 °C.

mixing time) decrease in radical absorbance corresponding to the reduction of 34 μM $ABTS^{\bullet-}$ (Figure 2, *ii*). This $ABTS^{\bullet-}$/NADH reaction stoichiometry of 1.9 was consistent with NADH functioning as a two e^- reductant. Importantly, 16 μM $ABTS^{\bullet-}$ was not reduced, and no further decreases in $[ABTS^{\bullet-}]$ occurred. Subsequent addition of 5 μM **Ru1** and 12.5 mM NAD^+ caused the radical absorbance to decrease to zero within 22 min, signifying complete reduction of the remaining $ABTS^{\bullet-}$ (Figure 2, *iii*). The ratio of NAD^+/NADH used in this experiment (694:1) was consistent with the ratio found in cells,[12−15] which demonstrates that, under conditions that exhausted the free cellular NADH supply, **Ru1** could utilize the substantially more abundant cellular stores of free NAD^+ to alleviate or prevent oxidative stress.

In the presence of horseradish peroxidase (HRP), addition of H_2O_2 to $ABTS^{2-}$ in PBS results in $ABTS^{\bullet-}$ formation, and the kinetics of this reaction can be used to evaluate the ability of an antioxidant to prevent or mitigate the onset of oxidative stress.[31] Inclusion of 5 μM **Ru1** and 25 mM NAD^+ significantly inhibited $ABTS^{\bullet-}$ formation, which never exceeded 4.8 μM (Figure 3A, red line). After 15 min, the radical absorbance began to decrease, and complete $ABTS^{\bullet-}$ reduction was observed 6.6 min later. In contrast, 5 μM NADH completely inhibited $ABTS^{\bullet-}$ formation for 3.3 min, whereupon the absorbance gradually increased to a maximum of 11 μM (Figure 3A, blue line). This concentration was 7 μM lower than the maximum observed in the control experiment and was consistent with NADH functioning as a two e^- reductant. The subsequent gradual decrease was due to normal $ABTS^{\bullet-}$ thermal decay.

After complete $ABTS^{\bullet-}$ reduction in the presence of **Ru1** was observed following the first H_2O_2 aliquot, two additional 10 μM H_2O_2 aliquots (#) were introduced and $[ABTS^{\bullet-}]$ peaked at 6.4 μM before being reduced completely each time (Figure 3B), demonstrating that the catalyst and terminal reductant were both still present and active. Different behavior was observed with NADH after $[ABTS^{\bullet-}]$ peaked. Adding a second H_2O_2 aliquot (#) caused $[ABTS^{\bullet-}]$ to increase to 17 μM (Figure 3C), corresponding to 94% $ABTS^{2-}$ oxidation (complete oxidation = 18 μM).[26] No change in absorbance was produced by the third H_2O_2 aliquot (#), consistent with all of the $ABTS^{2-}$ having been completely oxidized by the previous H_2O_2 aliquots. Subsequent treatment of this solution with 5 μM **Ru1** and 25 mM NAD^+ (§) resulted in complete $ABTS^{\bullet-}$ reduction within 45 min.

To demonstrate that the reactivity exhibited by **Ru1** and NAD^+ in Figure 3 derived specifically from $ABTS^{\bullet-}$ reduction, two 10 μM aliquots of chemically synthesized $ABTS^{\bullet-}$ (*) were added after the initial reaction with H_2O_2 was complete (Figure 4, red line). The $[ABTS^{\bullet-}]$ immediately increased by 8.8 μM

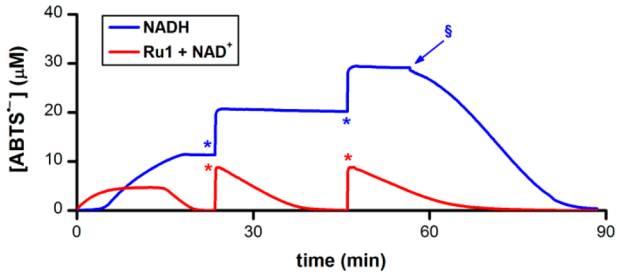

Figure 4. Plot of $[ABTS^{\bullet-}]$ vs time, which shows the oxidation of $ABTS^{2-}$ to $ABTS^{\bullet-}$ in situ by HRP and H_2O_2 followed by subsequent $ABTS^{\bullet-}$ reactivity in the presence of **Ru1** and NAD^+ (red line) or NADH (blue line). After the initial reaction of **Ru1** and NAD^+ or NADH had completed, two additional aliquots of 10 μM $ABTS^{\bullet-}$ (*) were introduced. For the NADH experiment (blue line), 5 μM **Ru1** and 25 mM NAD^+ were added (§) after the final aliquot of 10 μM $ABTS^{\bullet-}$. Conditions: $[HRP]_0$ = 10 nM, $[\mathbf{Ru1}]_0$ or $[NADH]_0$ = 5 μM, $[H_2O_2]_0$ = 10 μM, $[ABTS^{2-}]_0$ = 20 μM, $[NAD^+]_0$ = 25 mM, PBS (pH 7.4) at 25 °C.

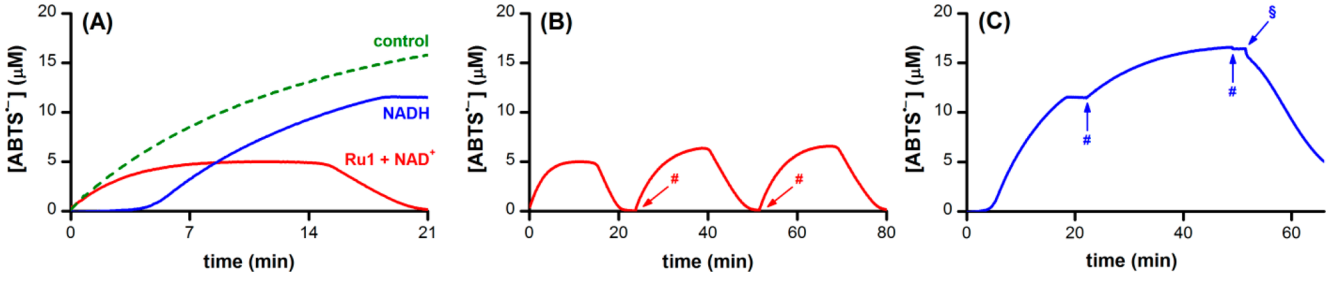

Figure 3. (A) Plot of $[ABTS^{\bullet-}]$ vs time, which shows the oxidation of $ABTS^{2-}$ to $ABTS^{\bullet-}$ in situ by HRP and H_2O_2 in the presence of **Ru1** and NAD^+ (red line), NADH (blue line), or **Ru1** without NAD^+ as a control (dotted green line). Plot of $[ABTS^{\bullet-}]$ vs time, which shows $ABTS^{\bullet-}$ formation following two additional aliquots of 10 μM H_2O_2 (#) in the presence of (B) **Ru1** and NAD^+ or (C) NADH. For the NADH experiment shown in (C), **Ru1** and NAD^+ were added (§) after the final aliquot of 10 μM H_2O_2. Conditions: $[HRP]_0$ = 10 nM, $[\mathbf{Ru1}]_0$ or $[NADH]_0$ = 5 μM, $[H_2O_2]_0$ = 10 μM, $[ABTS^{2-}]_0$ = 20 μM, $[NAD^+]_0$ = 25 mM, PBS (pH 7.4) at 25 °C.

DOI: 10.1021/jacs.6b10451
J. Am. Chem. Soc. 2016, 138, 15833−15836

each time, then decreased to zero 19 and 29 min after addition of the first and second $ABTS^{\bullet-}$ aliquots, respectively. We had previously shown that $ABTS^{2-}$ is an inhibitor for **Ru1**-catalyzed $ABTS^{\bullet-}$ reduction with nontertiary alcohols,[27] and given that the concentration of $ABTS^{2-}$ increased as each successive $ABTS^{\bullet-}$ aliquot was reduced, it was unsurprising that the time required for complete $ABTS^{\bullet-}$ reduction likewise increased. With the NADH experiment, however, the first and second $ABTS^{\bullet-}$ aliquots produced 9.4 and 9.3 μM increases in $[ABTS^{\bullet-}]$, respectively, that were stable over time (Figure 4, blue line). Subsequent addition of 5 μM **Ru1** and 25 mM NAD^+ (§) then achieved quantitative $ABTS^{\bullet-}$ reduction in less than 39 min.

In summary, NAD^+ is able to function as a terminal reductant for the **Ru1**-catalyzed reduction of $ABTS^{\bullet-}$ to $ABTS^{2-}$ in aerobic, aqueous solution. Because NAD^+ typically plays the role of H^- acceptor in biological systems, the classical expectation would be that it could not function as an H^- donor. However, the $ABTS^{\bullet-}$ reduction reactivity observed with NAD^+ and **Ru1** were highly conserved with our previous studies using other nontertiary alcohols as terminal reductants,[26,27] which suggested that the same mechanism was operative with NAD^+. The key intermediate responsible for $ABTS^{\bullet-}$ reduction with NAD^+ and **Ru1** was therefore inferred to be a Ru−H intermediate formed via β-hydride elimination from a ribose subunit coordinated to Ru, whereby this ability of NAD^+ to function as an H^- donor would give rise to its observed ability to function as a reductant. Previous studies by others have revealed that transition metal−hydride complexes formed via H^- transfer from NADH can react with atmospheric O_2 to generate H_2O_2,[32,33] which in turn can produce cytotoxic effects against cancer cells.[7−9,34−36] Given that free NAD^+ is 640−1100 times more abundant in cells than free NADH,[12−15] we believe that a catalyst that can utilize NAD^+ as an H^- source will be able to generate significantly higher H_2O_2 levels and thus exhibit substantially greater anticancer potency. The biological applications of **Ru1** will be detailed in subsequent reports.

■ ASSOCIATED CONTENT

Supporting Information

The Supporting Information is available free of charge on the ACS Publications website at DOI: 10.1021/jacs.6b10451.

Detailed experimental procedures, additional UV−visible spectra and kinetics plots (PDF)

■ AUTHOR INFORMATION

Corresponding Author

*atennys@clemson.edu

ORCID

Andrew G. Tennyson: 0000-0002-8593-2979

Notes

The authors declare no competing financial interest.

■ ACKNOWLEDGMENTS

This work was supported by the National Science Foundation (DMR-1555224). We thank Dr. A. Mangalum for prior work with **Ru1** and helpful discussions.

■ REFERENCES

(1) Borch, T.; Kretzschmar, R.; Kappler, A.; Van Cappellen, P.; Ginder-Vogel, M.; Voegelin, A.; Campbell, K. *Environ. Sci. Technol.* **2010**, *44*, 15−23.

(2) Falkowski, P. G.; Fenchel, T.; Delong, E. F. *Science* **2008**, *320*, 1034−1040.

(3) Hirst, J. *Annu. Rev. Biochem.* **2013**, *82*, 551−575.

(4) Nissen, M. S.; Youn, B.; Knowles, B. D.; Ballinger, J. W.; Jun, S.-Y.; Belchik, S. M.; Xun, L.; Kang, C. *J. Biol. Chem.* **2008**, *283*, 28710−28720.

(5) Talfournier, F.; Colloc'h, N.; Mornon, J.-P.; Branlant, G. *Eur. J. Biochem.* **1998**, *252*, 447−457.

(6) Deng, H.; Zheng, J.; Clarke, A.; Holbrook, J. J.; Callender, R.; Burgner, J. W., II *Biochemistry* **1994**, *33*, 2297−2305.

(7) Soldevila-Barreda, J. J.; Romero-Canelón, I.; Habtemariam, A.; Sadler, P. J. *Nat. Commun.* **2015**, *6*, 6582.

(8) Ritacco, I.; Russo, N.; Sicilia, E. *Inorg. Chem.* **2015**, *54*, 10801−10810.

(9) Liu, Z.; Sadler, P. J. *Acc. Chem. Res.* **2014**, *47*, 1174−1185.

(10) Fukuzumi, S.; Suenobu, T. *Dalton Trans.* **2013**, *42*, 18−28.

(11) Voss, C. V.; Gruber, C. C.; Faber, K.; Knaus, T.; Macheroux, P.; Kroutil, W. *J. Am. Chem. Soc.* **2008**, *130*, 13969−13972.

(12) Zhang, Q.; Piston, D. W.; Goodman, R. H. *Science* **2002**, *295*, 1895−1897.

(13) Hedeskov, C. J.; Capito, K.; Thams, P. *Biochem. J.* **1987**, *241*, 161−167.

(14) Veech, R. L.; Guynn, R.; Veloso, D. *Biochem. J.* **1972**, *127*, 387−397.

(15) Williamson, D. H.; Lund, P.; Krebs, H. A. *Biochem. J.* **1967**, *103*, 514−527.

(16) Kruger, N. J.; von Schaewen, A. *Curr. Opin. Plant Biol.* **2003**, *6*, 236−246.

(17) Besson, M.; Gallezot, P. *Catal. Today* **2000**, *57*, 127−141.

(18) Arts, S. J. H. F.; Mombarg, E. J. M.; van Bekkum, H.; Sheldon, R. A. *Synthesis* **1997**, *6*, 597−613.

(19) Saburi, M.; Ishii, Y.; Kaji, N.; Aoi, T.; Sasaki, I.; Yoshikawa, S.; Uchida, Y. *Chem. Lett.* **1989**, *18*, 563−566.

(20) A 3.3 μM decrease in $[ABTS^{\bullet-}]$ would produce a measurable change in absorbance (0.050), but a comparable absorbance change would require a 1.1 mM increase in $[H_2O_2]$. If a catalyst concentration of 5 μM is used, it would be possible to observe the reduction of less than 1 equiv of $ABTS^{\bullet-}$, but O_2 reduction would not be observable until more than 200 equiv of H_2O_2 had been produced.

(21) In aqueous buffer, ε = 15,000 M^{-1} cm^{-1} at λ = 734 nm for $ABTS^{\bullet-}$ vs ε = 43.6 M^{-1} cm^{-1} at λ = 240 nm for H_2O_2.

(22) Re, R.; Pellegrini, N.; Proteggente, A.; Pannala, A.; Yang, M.; Rice-Evans, C. *Free Radical Biol. Med.* **1999**, *26*, 1231−1237.

(23) Yusa, K.; Shikama, K. *Biochemistry* **1987**, *26*, 6684−6688.

(24) Scott, S. L.; Chen, W.-J.; Bakac, A.; Espenson, J. H. *J. Phys. Chem.* **1993**, *97*, 6710−6714.

(25) Jungwirth, U.; Kowol, C. R.; Keppler, B. K.; Hartinger, C. G.; Berger, W.; Heffeter, P. *Antioxid. Redox Signaling* **2011**, *15*, 1085−1127.

(26) Htet, Y.; Tennyson, A. G. *Chem. Sci.* **2016**, *7*, 4052−4058.

(27) Htet, Y.; Tennyson, A. G. *Angew. Chem., Int. Ed.* **2016**, *55*, 8556−8560.

(28) Achrainer, F.; Emel'yanenko, V. N.; Tantawy, W.; Verevkin, S. P.; Zipse, H. *J. Phys. Chem. B* **2014**, *118*, 10426−10429.

(29) Achrainer, F.; Zipse, H. *Molecules* **2014**, *19*, 21489−21505.

(30) Sen, S.; Pal, U.; Maiti, N. C. *J. Phys. Chem. B* **2014**, *118*, 909−914.

(31) Pitulice, L.; Pastor, I.; Vilaseca, E.; Madurga, S.; Isvoran, A.; Cascante, M.; Mas, F. *J. Biocatal. Biotransformation* **2013**, *2*, 1−5.

(32) Suenobu, T.; Shibata, S.; Fukuzumi, S. *Inorg. Chem.* **2016**, *55*, 7747−7754.

(33) Maid, H.; Böhm, P.; Huber, S. M.; Bauer, W.; Hummel, W.; Jux, D. N.; Gröger, H. *Angew. Chem., Int. Ed.* **2011**, *50*, 2397−2400.

(34) Liu, Z.; Romero-Canelón, I.; Qamar, B.; Hearn, J. M.; Habtemariam, A.; Barry, N. P. E.; Pizarro, A. M.; Clarkson, G. J.; Sadler, P. J. *Angew. Chem., Int. Ed.* **2014**, *53*, 3941−3946.

(35) Fu, Y.; Romero, M. J.; Habtemariam, A.; Snowden, M. E.; Song, L.; Clarkson, G. J.; Qamar, B.; Pizarro, A. M.; Unwin, P. R.; Sadler, P. J. *Chem. Sci.* **2012**, *3*, 2485−2494.

(36) Dougan, S. J.; Habtemariam, A.; McHale, S. E.; Parsons, S.; Sadler, P. J. *Proc. Natl. Acad. Sci. U. S. A.* **2008**, *105*, 11628−11633.

DOI: 10.1021/jacs.6b10451
J. Am. Chem. Soc. 2016, 138, 15833−15836